

## 1. History of high entropy oxides

The concept of high-entropy materials has been one of the most influential ones in the materials science during the last decade. It started in 1995 with the development of the first high-entropy alloys (HEAs) by Yeh and Huang [1], however, it was not fully appreciated until 2004 when articles by Yeh *et al.* [2] and Cantor *et al.* [3] triggered the worldwide studies on the subject. Today, the idea of multicomponent, entropy-stabilized solid solutions is not limited just to metallic materials, but was successfully applied to other groups as well, such as high-entropy alloy nitrides (HEANs) [4], carbides (HECs) [5, 6], diborides (HEBs) [7] and oxides (HEOx) [8].

The high-entropy alloys remain the most studied group of high-entropy materials and in fact are considered to be the benchmark for other groups, as most of the concepts used in the development of HEAs can be, at least to some degree, translated to them. In fact, the high-entropy alloys remain the only group, for which a definition was agreed. The most common definition states [2] that they are alloys with 5 or more (often the upper limit is arbitrary set to 13) principal elements. Each principal element should have a concentration between 5 and 35 at.%. The configurational entropy of such a system reaches the maximum for a solid solution phase, favoring formation of simple crystal structures. While today the definition seems to be loosened, as 4-component systems are also sometimes counted among HEAs [9-11], it certainly shows the essence of the whole concept. The extremely fast dynamics of HEAs development results from their unusual properties, which were categorized by Yeh [12] into four core effects:

- Thermodynamics: high entropy effects - high configurational entropy tends to stabilize solid solution phases
- Kinetics: sluggish diffusion - kinetics of diffusion is slower than in conventional alloys and pure metals
- Structure - severe lattice distortion - atoms are randomly distributed in the crystal lattice, leading to its distortion and affecting mechanical, transport and thermal properties
- Properties: cocktail effect - synergistic effect resulting from mutual interactions among composing elements, which would bring excess quantities to the average values simply predicted by the mixture rule

While the extent or even existence of these effects has been a subject of discussions [13, 14], they can be considered a driving force of the studies of high-entropy materials. Above effects originate from the most basic thermodynamic and structural properties, therefore, it can be expected that their applicability is not limited just to metallic systems, but to other materials sharing the same design principles as well.

The analogy to high-entropy alloys was the main inspiration for the group of Rost *et al.* during the development of the first high-entropy oxide material [8] (named by the authors as an "entropy-stabilized oxide"). As a result of their studies, they obtained a single-phased, Rocksalt-structured ( $Fm\bar{3}m$ ) (Co,Cu,Mg,Ni,Zn)O solid solution. The choice of the composing elements, far from optimal one as both ZnO and CuO are characterized by respectively Wurtzite and Tenorite structures, was based on the motivation "*to provide the appropriate diversity in structures, coordination and cationic radii to test directly the entropic ansatz.*". The material was synthesized through free sintering of the composing oxides followed by quenching. The material stability was studied at various temperatures showing a reversible, endothermic, entropy-driven phase transition at a temperature of 900°C, over which it exhibited the mentioned single-phase Rocksalt structure. The randomness of the ions distribution was confirmed by the X-ray absorption fine structure method (EXAFS), showing the lack of both short- and long-range order. All quaternary, equimolar subsystems of the (Co,Cu,Mg,Ni,Zn)O

were studied, showing that it was impossible to stabilize the single-phase structures in systems characterized by lower configurational entropy.

The aforementioned study was a part of the Rost PhD thesis [15], in which a much wider spectrum of compositions was tested. Most of them resulted in the multiphase mixtures. However, some of them exhibited a single-phase structure, showing the feasibility of the whole idea. The summary of the single-phase systems obtained by Rost is presented in Table 1.

Table 1. Single phase structures synthesized by Rost [15] (free sintering in air at 1000°C / 24 hrs).

<b>HEOx single phase structures</b>	
Mg-Cu-Fe-Zn-Ti-O	Ni-Cu-Ga-Zn-Ti-O
Al-Fe-Cr-Mn-Ni-O	Ga-Fe-Cr-Mn-Ni-O
Mg-Ni-Mn-Fe-Co-O	Al-Fe-Cr-Mn-Ni-O
Mg-Ni-Cu-Zn-Co-O	

The studies on the properties of high-entropy oxide systems were started by the Bérardan *et al.* who investigated the electrical properties of the (Co,Cu,Mg,Ni,Zn)O and doping effect of other cations [16, 17]. In their first study [16] the authors examined the possibility of doping the base structure with various 1<sup>+</sup>, 3<sup>+</sup> and 4<sup>+</sup> cations (respectively Li<sup>+</sup>, In<sup>3+</sup>, Ga<sup>3+</sup> and Ti<sup>4+</sup> ions). As a result, it turned out that the presence of cations characterized by higher valence, destabilized the structure leading to the formation of multiphase mixtures with the influence of high configurational entropy being overwhelmed by other interactions. The addition of the Li<sup>+</sup> however, proved to be successful, allowing to preserve a single-phase structure. To explain this phenomenon a compensating mechanism, involving the presence of Co<sup>3+</sup> or/and oxygen vacancies, was postulated, with Co<sup>3+</sup> peaks being visible on the XPS (X-ray photoelectron spectroscopy) spectra of doped samples. Additionally, a co-substitution with Li<sup>+</sup> and Ga<sup>3+</sup> was performed, again leading to a single-phase (Co,Cu,Mg,Ni,Zn)<sub>1-2x</sub>Li<sub>x</sub>Ga<sub>x</sub>O solid solutions, further confirming the presence of compensating mechanism. The electrical studies were performed for the equimolar (Co,Cu,Mg,Ni,Zn)O and (Co,Cu,Li,Mg,Ni,Zn)O materials. Both materials exhibited a semiconductor-like behavior with the relatively big difference in their resistivity, what can be explained by the formation of electroactive defects in the material doped with Li. For the (Co,Cu,Mg,Ni,Zn)<sub>0.95</sub>Li<sub>0.05</sub>O measurements of the relative permittivity were performed (440 K, frequency of 20 Hz) showing the colossal dielectric constant values of 2·10<sup>5</sup>. This property was deemed by the authors to be characteristic for the HEOx phase.

The second study of Bérardan *et al.* [17] focused on the measurements of the electronic and ionic conductivities of the (Co,Cu,Mg,Ni,Zn)O doped with different level of Li, Na, K and both Li and Ga. The authors also tested the upper limit of dopants' content, which permitted to preserve the single-phase structure of the materials. The determined values were 33%, 15%, 5% and 7.5/7.5% for Li, Na, K, and Li/Ga respectively. The measured electronic conductivities of (Co,Cu,Mg,Ni,Zn)O and (Co,Cu,Mg,Ni,Zn)<sub>0.7</sub>Li<sub>0.3</sub>O, were  $\sigma_e = 2 \cdot 10^{-9} \text{ S} \cdot \text{cm}^{-1}$ , making both materials the electrical insulators. The studies of the ionic conductivity were carried out by means of electrochemical impedance spectroscopy method (EIS), in a function of dopants' content. The results shown in Fig. 1., were nothing short of spectacular, with the samples being doped with 30% of Li significantly outperforming the state-of-the-art LiPON (lithium phosphorous oxy-nitride) solid electrolyte by orders of magnitude at 20 and 80 °C. Also, the sample with 15% of Na performed similarly or better than LiPON, considerably exceeding its ionic conductivity at 20 °C.

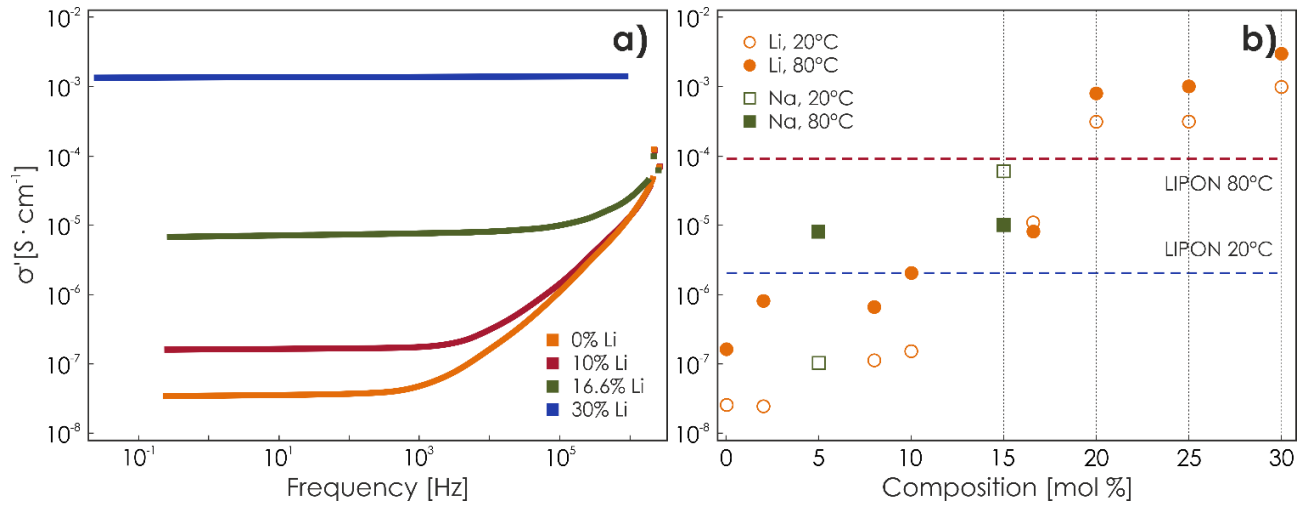


Fig. 1. Ionic conductivities of: a) Li doped samples at room temperature measured in a function of frequency; b) Li and Na doped HEOx samples compared with the LiPON's performance [17].

The working theory presented by the authors was that small alkali ions were moving through the oxygen vacancies that were incorporated into the matrix during their synthesis, as a part of the charge compensating mechanism. The samples with potassium as the dopant, and co-doped with Li and Ga exhibited much lower values of ionic conductivity, most probably due to relatively too big radius of  $K^+$  ions and much lower concentration of the oxygen vacancies in the material with  $Ga^{3+}$  ions.

The compensation mechanism in doped (Co,Cu,Mg,Ni,Zn)O was further studied by Rak *et al.* [18] by means of DFT (density functional theory) calculations followed by the experimental verification. The studies showed on the example of  $Sc^{3+}$  ions that there is a possibility to introduce the ions of higher valence without losing the single-phase structure, what stands in contrary to the results of Bérardan *et al.* [16]. According to the results by Rak *et al.*, the introduction of ions with formal charges of either  $1^+$  and  $3^+$  always results in the pronounced charge transfer to other ions in the system, what is reflected by their effective Bader charges being considerably different to those observed in binary compositions. The authors also indicated that contrary to the situation observed in high entropy alloys, in the case of HEOx materials the formulation of the empirical rules, which could govern the process of composing materials selection, may be extremely difficult.

The latest studies on the subject of (Co,Cu,Mg,Ni,Zn)O focused on the influence of Cu on its atomic structure [19, 20], and influence of synthesis method on the microstructure of (Co,Cu,Mg,Ni,Zn)O and (Co,Mg,Ni,Zn)O [21]. The groups of Berardan *et al.* [19] and Rost *et al.* [20] independently showed, by means of different methods, that the presence of Cu cations within the structure of (Co,Cu,Mg,Ni,Zn)O leads to distortion of the anionic sublattice, consistent with the Jahn-Teller origins. In the case of studies by Berardan *et al.* [19] the authors analyzed the deviation of the XRD peaks intensity ratio from the ideal behavior. It was shown that it partially depends on the cooling rate during quenching and thermal history of the sample, but the main reason for such behavior was the influence of Cu cations, studied by the preparation of a number of samples with Cu content varying from 16 to 28 at.%. It was postulated that the evolution of the local environment of the  $Cu^{2+}$  ions from octahedral to rhombic takes place. Finally, the authors studied the influence of the considered deviations from the ideal structure on the electric properties, showing a strong correlation. It may indicate that the properties of the HEOx materials can be easily tailored through the small variations of composition. The detailed studies of the same material conducted by Rost *et al.* [20] using EXAFS method led to similar conclusions, as the length of Cu-O bond differed significantly from the other bonds in the system, showing also a relatively big variation. The last study published up

to this day was conducted by Sarkar *et al.* [21]. The authors obtained the (Co,Cu,Mg,Ni,Zn)O and (Co,Mg,Ni,Zn)O by means of three different methods: nebulised spray pyrolysis (NSP), flame spray pyrolysis (FSP) and reverse co-precipitation (RCP). The results showed that the microstructure of the obtained materials strongly depended on the method of synthesis and its temperature, as the authors were able to obtain single-phase (Co,Mg,Ni,Zn)O using the NSP method at temperature of 1250 °C, what is in contrary to the reports of Rost *et al.* [8], who, however, used a lower temperature of 1000 °C at which the stabilizing effect of the entropy was less pronounced.

It is worth noting that the choice of structures in transition-metal HEO<sub>x</sub> (TM-HEO<sub>x</sub>) is not limited to just Rocksalt structures. Recent findings by Dąbrowa *et al.* [22] showed the possibility of spinel phase formation in HEO<sub>x</sub>. The homogeneity of the (Co,Cr,Fe,Mn,Ni)<sub>3</sub>O<sub>4</sub> *Fd-3m* spinel was proved with use of XRD, SEM+EDS, and Raman spectroscopy methods. Therefore, it can be expected that the available palette of the TM-HEO<sub>x</sub> will grow rapidly in the nearest future.

Another group of HEO<sub>x</sub> is fluorite-structured high entropy oxides. They can be considered as a sort of a further development of doped ceria Ce<sub>1-x</sub>RE<sub>x</sub>O<sub>2-x/2</sub>, doped zirconia (ZrO<sub>2</sub>)<sub>1-x</sub>(RE<sub>2</sub>O<sub>3</sub>) and doped hafnia (HfO<sub>2</sub>)<sub>1-x</sub>(RE<sub>2</sub>O<sub>3</sub>)<sub>x</sub> materials, a group, which includes some of the most promising oxygen ion conducting solid electrolytes, essential for successful operation of solid oxide fuel cells (SOFCs) and solid oxide electrolyser cells (SOEC) [23-25]. The first study in this area was presented in 2016 by Djenadic *et al.* [26]. The authors synthesized a number of different compositions based on the equimolar mixtures of ceria and different RE oxides, obtaining a number of 3 - 6 component systems, including high entropy: (Ce,La,Pr,Sm,Y)O<sub>2-δ</sub>, (Ce,La,Nd,Pr,Sm,Y)O<sub>2-δ</sub> and (Ce,Gd,La,Nd,Pr,Sm,Y)O<sub>2-δ</sub> ("multicomponent rare earth oxides"). In all cases, the as-received materials were characterized by a single phase, fluorite, *Fm-3m* solid solution structure. However, after reequilibrating at 1000 °C, followed by slow cooling with the furnace, the symmetry of most of the systems was reduced to the *Ia-3* structure, most probably due to the presence of vacancy ordering effect, similarly as *e.g.* in ceria doped with Gd<sub>2</sub>O<sub>3</sub> [27]. The single-phase structures were observed only in systems with cerium (even for the ternary systems), what suggests different mechanisms of solid-solution formation and charge compensation than the ones observed by Rost *et al.* [8], and highlights the role of CeO<sub>2</sub> as a parent structure. The oxidation states of Ce and Pr in both as-received and annealed materials were investigated with use of XPS, with the results suggesting the presence of Ce<sup>4+</sup> ions only, and mixed oxidation state of Pr ions (both Pr<sup>3+</sup> and Pr<sup>4+</sup>) in both types of the materials.

The same group published another study on this subject in 2017 [28], focused on the band structure of the previously obtained REO<sub>x</sub>. Again, both as-received (*Fm-3m*) and calcined (*Ia-3*) samples were considered. The XPS measurements were extended on all elements in the systems, showing that all of them, except for Ce<sup>4+</sup> and Pr<sup>3+</sup>/Pr<sup>4+</sup>, had a 3<sup>+</sup> oxidation state. As a consequence, all REO<sub>x</sub> were deemed to be characterized by an extremely high amount of oxygen vacancies (up to 19% of anionic sites being empty in the most extreme cases), what was further indirectly confirmed with use of Raman spectroscopy. The band gap values of different REO<sub>x</sub> compositions were similar, with an average value of direct  $E_g$  of about 2.06 eV, significantly smaller than 3.17 eV measured for pure CeO<sub>2</sub>.

The most recent studies concerning the fluorite-structured HEO<sub>x</sub> present a different approach to the topic, using all 3 basic oxides: CeO<sub>2</sub>, HfO<sub>2</sub>, and ZrO<sub>2</sub> simultaneously. Chen *et al.* [29] obtained an almost single-phase, fluorite-structured (Ce,Zr,Hf,Sn,Ti)O<sub>2</sub> solid solution, in which all elements, except for Ce, exhibited a uniform distribution. During electrical conductivity measurements, a relatively high value of energy of activation  $E_a$  of 1.43 eV was determined for the 600-1100 °C temperature range. The measured room temperature thermal conductivity was 1.28 Wm<sup>-1</sup>K<sup>-1</sup>, roughly 50% of that observed for the 7 wt.% yttria-stabilized zirconia (7YSZ). The same direction of studies

was followed by the group of Gild *et al.* [30], who doped the equimolar composition of (Ce,Hf,Zr) with combinations of Ti, Y, Yb, La, Gd, Ca and Mg ions, obtaining a number of different fluorite-structured materials. The conclusions concerning the thermal conductivity were similar as in the case of Chen *et al.*, while the electrical conductivity was deemed to be an order of magnitude lower than in 8YSZ, with  $E_a$  varying from 1.14-1.29 eV.

Similarly as in the case of TM-HEOx, the fluorite-structured, or rather rare-earth high entropy oxides, are not limited strictly to the fluorite  $Fm-3m$  space group and its less symmetric counterparts. It has already been proved that combined with other ions of suitable ionic radii, e.g. TM or alkaline cations, they can form perovskite structures [31, 32], what should greatly expand the range of their potential applications.

## 2. Electrical measurements

Looking at the history of the high entropy oxides, it becomes clear that their potentially most promising properties are the electrical ones. Therefore, the electrical measurements are of extremely high priority in this particular group of materials.

The starting point of all electrical considerations is the Ohm's law:

$$R = \frac{U}{I}, \quad (1.1)$$

where  $R$  denotes resistivity,  $U$  - potential and  $I$  - current. The problem is that in this independent from frequency form of law, the only one type of circuit element can be described - the resistor. Of course, the real materials rarely have such character. That is why often another form of Ohm's law is used:

$$Z(\omega) = \frac{U(\omega)}{I(\omega)}, \quad (1.2)$$

where  $Z$  denotes impedance and  $\omega$  is the radial frequency. Usually, the alternating potential and current have a sinusoidal character:

$$\begin{aligned} U(\omega) &= U_0 \sin(\omega t) \\ I(\omega) &= I_0 \sin(\omega t + \delta) \end{aligned} \quad (1.3)$$

where  $\delta$  is the phase shift, between the potential signal and current response. Alternatively, we can present the functions from (1.3) in exponential form:

$$\begin{aligned} U(\omega) &= U_0 \exp(i\omega t) \\ I(\omega) &= I_0 \exp(i(\omega t - \delta)) \end{aligned} \quad (1.4)$$

As a result:

$$Z(\omega) = \frac{U(\omega)}{I(\omega)} = Z_0 \exp(i\delta) = Z_0 (\cos \delta + i \sin \delta) = Z'(\omega) + Z''(\omega), \quad (1.5)$$

where:  $Z'(\omega)$  - resistivity,  $Z''(\omega)$  - reactance

Depending on the type of the signal we use, it is possible to conduct electrical measurements in various variants. In general, there are 3 main types of electrical measurements which have to be considered. Each of them offers both advantages and disadvantages:

- **Direct current measurements (DC)** - the most basic of the methods

- + easy to carry out
- + simple apparatus
- + easy interpretation
- a limited amount of information
- measures only the real part of the impedance
- can lead to the formation of an electrical double layer on the sample/electrode interface

- **Alternating current (AC)** - in ideal case it should give the same results as DC

- + easy to carry out
- + simple apparatus
- + easy interpretation
- + smaller probability of double layer formation than in DC
- a limited amount of information
- measures only the real part of the impedance

- **Electrochemical Impedance Spectroscopy (EIS)**

- + offers a huge variety of information
- + allows separating contributions from different mechanisms of conductivity
- + measures real and imaginary parts of impedance, as well as the phase shift
- requires a much more advanced technical base
- interpretation of the results is often not straightforward and unambiguous
- extremely time consuming

In general, the electrochemical impedance spectroscopy is by far the most informative method. As a result of the measurement, one can obtain information on both resistivity and reactance, as well as phase shift. On the other hand, it is an extremely complex method with high technical requirements, making the AC/DC measurements an interesting alternative.

The AC and DC values can be considered specific cases of the impedance measurements. Let's consider the most typical type of circuit in materials measurement, the parallel R-C circuit:

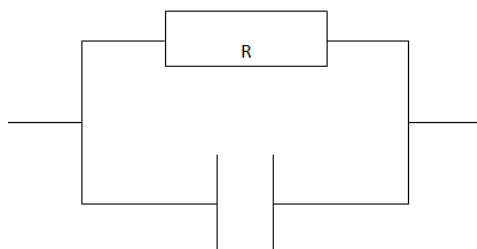


Fig. 2. R-C parallel circuit.

The impedance spectra of such a circuit look as follows:

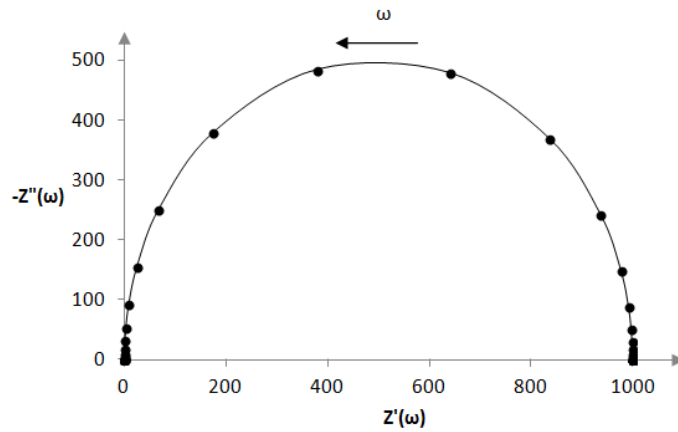


Fig.3. The impedance spectra of the R-C circuit.

With the impedance spectroscopy, we are able to measure the whole range of  $\omega$ , obtaining the whole semi-circle. With the DC method, in fact we are measuring only the one point, namely the  $\omega \rightarrow 0$ . The AC method measures on the other hand point of specific  $\omega$ , which however, usually is low enough to make the obtained value of R practically equal to the DC value. What is worth remembering, with the AC method, despite the sinusoidal signal, we do not get any information concerning the reactance.

For each type of measurement, we can use a different type of measuring circle. The 3 most common types are:

- 2 - point probe method
- 4 - point probe method
- quasi 4 - point probe method

**The 2 - point probe method** is the simplest one - we simply put the electrodes on the separate end of the sample, apply the current and measure the potential's decrease. The equivalent circuit for this method is as follows:

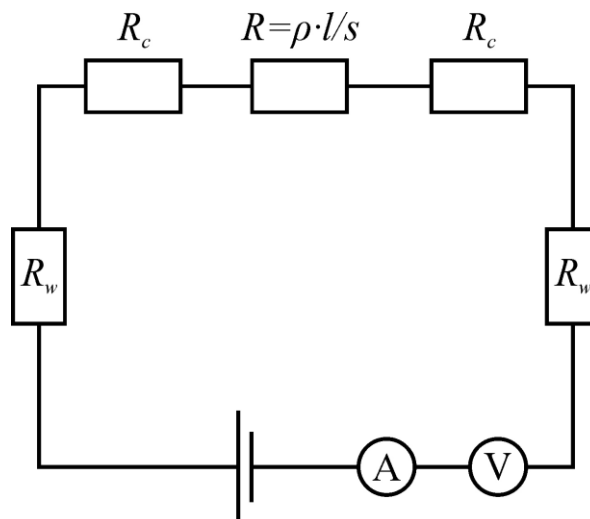


Fig. 4. 2 - point probe method equivalent circuit

The main problem with this method is the fact, that we are measuring the resistivity/impedance of everything - sample, electrodes, wires *etc.*

The opposite end of the spectrum is the **4 - point probe method**. In this method, another circuit, attached directly to the sample is created:

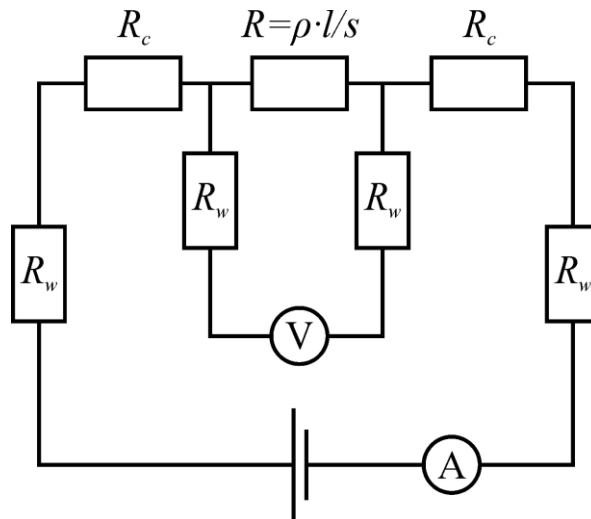


Fig. 5. 4 - point probe method equivalent circuit

Thanks to this, we are able to measure only the sample, with other components of the circuit being dismissed. On the other hand, the 4 - point probe method is quite demanding from the experimental point of view, requiring wiring of each measured sample and limiting the possible shapes and sizes of the measured material.

A reasonable compromise is the **quasi 4 - point probe method** in which the measuring, much shorter circuit is attached to the sample, but outside of electrodes. As a result, we are greatly reducing the influence of the main wires.

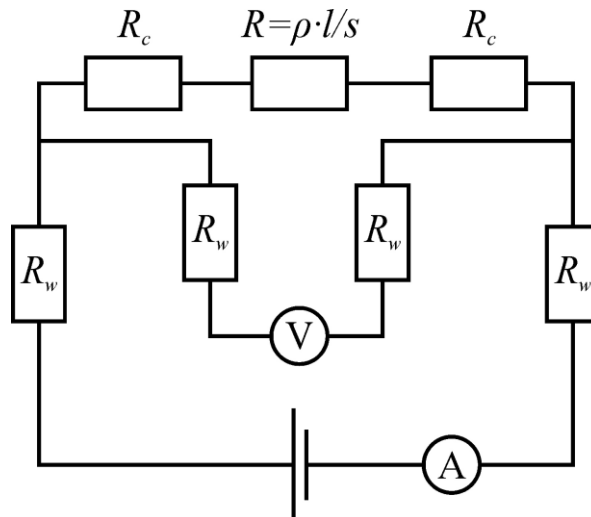


Fig. 6. quasi 4 - point probe method equivalent circuit.

### 3. Determining the conductivity

The most basic relation between conductivity  $\sigma$  and resistivity is as follows:

$$\sigma = \frac{l}{SR}, \tag{1.6}$$



where:  $l$  - thickness of the sample,  $S$  - area,  $R$  - resistivity. Since the conductivity in semiconductors (the materials we are considering) is a thermally activated process, its temperature dependence can be described by the Arrhenius-type relation of the following form:

$$\sigma T = \sigma_0 \exp\left(-\frac{E_a}{RT}\right), \quad (1.7)$$

where  $E_a$  is the energy of activation,  $R$  - gas constant and  $\sigma_0$  is the preexponential constant. The values of energies of activation are dependent on phase, the mechanism of conductivity and many, many more factors.

#### 4. Literature

- [1] K. H. Huang and J. W. Yeh, A study on multicomponent alloy systems containing equal-mole elements 1996
- [2] J. W. Yeh, S. K. Chen, S. J. Lin, J. Y. Gan, T. S. Chin, T. T. Shun, C. H. Tsau and S. Y. Chang, Nanostructured high-entropy alloys with multiple principal elements: novel alloy design concepts and outcomes. *Advanced Engineering Materials* 2004 Vol. 6 pp. 299-303
- [3] B. Cantor, I. T. Chang, P. Knight and A. J. Vincent, Microstructural development in equiatomic multicomponent alloys. *Materials Science and Engineering: A* 2004 Vol. 375-377 pp. 213-218
- [4] T.K.Chen, T. T. Shun, J. W. Yeh and M. S. Wong, Nanostructured nitride films of multi-element high-entropy alloys by reactive DC sputtering. *Surface and Coatings Technology* 2004 Vol. 188-189 pp. 193-200
- [5] J. Zhou, J. Zhang, F. Zhang, B. Niu, L. Lei and W. Wang, High-entropy carbide: A novel class of multicomponent ceramics. *Ceramics International* 2018 Vol. 44 pp. 22014-22018
- [6] E. Castle, T. Csanadi, S. Grasso, J. Dusza and M. Reece, Processing and Properties of High-Entropy Ultra-High Temperature Carbides. *Scientific Reports* 2018 Vol. 8 pp. 8609
- [7] J. Gild, Y. Zhang, T. Harrington, S. Jiang, T. Hu, M. X. Quinn, W. M. Mellor, N. Zhou, K. Vecchio and J. Luo, High-Entropy Metal Diborides: A New Class of High-Entropy Materials and a New Type of Ultrahigh Temperature Ceramics. *Scientific Reports* 2016 Vol. 6 pp. 37946
- [8] C. M. Rost, R. Schaet, T. Borman, A. Moballegh, E. C. Dickey, D. Hou, J. L. Jones, S. Curtarolo and J. P. Maria, Entropy-stabilized oxides. *Nature Communications* 2015 Vol. 6 pp. 8485
- [9] Ł. Rogal, J. Morgiel, Z. Świątek and F. Czerwiński, Microstructure and mechanical properties of the new Nb<sub>25</sub>Sc<sub>25</sub>Ti<sub>25</sub>Zr<sub>25</sub> eutectic high entropy alloy. *Materials Science and Engineering A* 2016 Vol. 651 pp. 590-597
- [10] S. Praveen, J. Basu, S. Kashyap and R. S. Kottada, Exceptional resistance to grain growth in nanocrystalline CoCrFeNi high entropy alloy at high temperature. *Journal of Alloys and Compounds* 2016 Vol. 662 pp. 361-367
- [11] Z. Li, K. G. Pradeep, Y. Deng, D. Raabe and C. C. Tasan, Metastable high-entropy dual-phase alloys overcome the strength-ductility trade-off. *Nature* 2016 Vol. 534 pp. 227-230
- [12] J. W. Yeh, Recent Progress in High-entropy Alloys. *Annales de Chimie-Science des Materiaux* 2006 Vol. 31 pp. 633-648
- [13] E. J. Pickering and N. G. Jones, High-entropy alloys: a critical assessment of their founding principles and future prospects. *International Materials Reviews* 2016 Vol. 61 pp. 183-202
- [14] D. B. Miracle and O. N. Senkov, A critical review of high entropy alloys and related concepts. *Acta Materialia* 2017 Vol. 112 pp. 448-511
- [15] C. M. Rost, Entropy-Stabilized Oxides: Explorations of a Novel Class of Multicomponent Materials. North Carolina State University, 2016

- [16] F. S. Bérardan D., Dragoë D., Meena A.K., Dragoë N., Colossal dielectric constant in high entropy oxides. *Physica Status Solidi rapid research letters* 2016 Vol. 10 pp. 328-333
- [17] F. S. Bérardan D., Meena A.K., Dragoë D., Room temperature lithium superionic conductivity in high entropy oxides. *Journal of Materials Chemistry A* 2016 Vol. 4 pp. 9536-9541
- [18] Z. Rak, C. M. Rost, M. Lim, P. Sarker, C. Toher, S. Curtarolo, J. P. Maria and D. W. Brenner, Charge compensation and electrostatic transferability in three entropy-stabilized oxides: Results from density functional theory calculations. *Journal of Applied Physics* 2016 Vol. 120 pp.
- [19] Berardan D., Meena A. K., Franger S., Herrero C. and D. N., Controlled Jahn-Teller distortion in (MgCoNiCuZn)O-based high entropy oxides. *Journal of Alloys and Compounds* 2017 Vol. 704 pp. 693-700
- [20] Rost C.M., Rak Z., Brenner D.W. and M. J.P., Local structure of the  $Mg_xNi_xCo_xCu_xZn_xO(x=0.2)$  entropy-stabilized oxide: An EXAFS study. *Journal of the American Ceramic Society* 2017 Vol. 100 pp. 2732-2738
- [21] Sarkar A., Djenadic R., Usharani N.J., Sanghvi K.P., Chakravadhanula V.S.K., Gandhi A.S., Hahn H. and B. S.S., Nanocrystalline multicomponent entropy stabilised transition metal oxides. *Journal of the European Ceramic Society* 2017 Vol. 37 pp. 747-754
- [22] J. Dąbrowa, M. Stygar, A. Mikuła, A. Knapik, K. Mroczka, W. Tejchman, M. Danielewski and M. Martin, Synthesis and microstructure of the (Co,Cr,Fe,Mn,Ni)<sub>3</sub>O<sub>4</sub> high entropy characterized by spinel structure. *Materials Letters* 2018 Vol. 216 pp. 32-36
- [23] M. Mogensen, N. M. Sammes and G. A. Tompsett, Physical, chemical and electrochemical properties of pure and doped ceria. *Solid State Ionics* 2000 Vol. 129 pp. 63-94
- [24] O. Yamamoto, Solid oxide fuel cells: fundamental aspects and prospects. *Electrochimica Acta* 2000 Vol. 45 pp. 2423-2435
- [25] M. F. Trubelja and V. S. Stubican, Ionic Conductivity of the Fluorite-type Hafnia-R<sub>2</sub>O<sub>3</sub> Solid Solutions. *Journal of the American Ceramic Society* 1991 Vol. 74 pp. 2489-2494
- [26] R. Djenadic, A. Sarkar, O. Clemens, C. Loho, M. Botros, V. S. K. Chakravadhanula, C. Kübel, S. S. Bhattacharya, A. S. Gandhi and H. Hahn, Multicomponent equiatomic rare earth oxides. *Materials Research Letters* 2016 Vol. 5 pp. 102-109
- [27] A. Kossov, Q. Wang, R. Korobko, V. Grover, Y. Feldman, E. Wachtel, A. K. Tyagi, A. I. Frenkel and I. Lubomirsky, Evolution of the local structure at the phase transition in CeO<sub>2</sub>-Gd<sub>2</sub>O<sub>3</sub> solid solutions. *Physical Review B* 2013 Vol. 87 pp. 054101
- [28] A. Sarkar, C. Loho, L. Velasco, T. Thomas, S. S. Bhattacharya, H. Hahn and R. R. Djenadic, Multicomponent equiatomic rare earth oxides with a narrow band gap and associated praseodymium multivalency. *Dalton transactions* 2017 Vol. 46 pp. 12167
- [29] K. Chen, X. Pei, L. Tang, H. Cheng, Z. Li, C. Li, X. Zhang and L. Ad, A five-component entropy-stabilized fluorite oxide. *Journal of the European Ceramic Society* 2018 Vol. 38 pp. 4161-4164
- [30] J. Gild, M. Samiee, J. L. Braun, L. Braun, T. Harrington, H. Vega, P. E. Hopkins, K. Vecchio and J. Luo, High-entropy fluorite oxides. *Journal of the European Ceramic Society* 2018 Vol. 38 pp. 3578-3584
- [31] A. Sarkar, R. Djenadic, D. Wang, C. Hein, R. Kautenburger, O. Clemens and H. Hahn, Rare earth and transition metal based entropy stabilised perovskite type oxides. *Journal of the European Ceramic Society* 2018 Vol. 38 pp. 2318-2327
- [32] S. Jiang, T. Hu, J. Gild, N. Zhou, J. Nie, M. Qin, T. Harrington, K. Vecchio and J. Luo, A new class of high-entropy perovskite oxides. *Scripta Materialia* 2018 Vol. 142 pp. 116-120